A sequence stratigraphic framework for the Upper Devonian Woodford Shale, Permian Basin, west Texas

Nikki T. Hemmesch[1], Nicholas B. Harris[*2,1], Cheryl A. Mnich[1,3], and David Selby[4]

[1] Department of Geology and Geological Engineering, Colorado School of Mines, Golden, CO

[2] Department of Earth and Atmospheric Sciences, University of Alberta, Edmonton, Canada

[3] Now at: ConocoPhillips Inc., Houston, TX

[4] Department of Earth Sciences, Durham University, Durham, U.K.

* corresponding author: nharris@ualberta.ca

1 ABSTRACT

Criteria for recognizing stratigraphic sequences are well established on continental margins but much more challenging in basinal settings. Current paradigms rely primarily on assignment of high gamma ray intervals to transgressive systems tracts or maximum flooding surfaces and the somewhat controversial delineation of exposure surfaces in cores. This study of the Upper Devonian Woodford Shale, Permian Basin, west Texas, attempts to identify sea level signatures in an organic-shale through detailed sedimentological analysis of long cores.

The Woodford is a prominent source of hydrocarbons and a target for shale gas reserves In the Permian basin. The formation is dominated by organic-rich mudstone, with interbeds of non-mudstone lithofacies including carbonate beds, chert beds and radiolarian laminae, all probably deposited as sediment gravity flows. Overlying the organic-rich mudstone in one well is a thick bioturbated organic-poor mudstone that indicates overall shallowing-up, consistent with a 2nd order global eustatic sea level fall from 386 to 359 Ma. Carbonate beds occur in bundles that define a cyclicity typically 5 to 10 meters thick; these are interpreted as reflecting high stand shedding. Thus intervals of interbedded carbonate and organic-rich mudstone define 3rd order high stands, while the intervening intervals of uninterrupted organic-rich mudstone mark low stand and transgressive systems tracts. Chert beds are concentrated in the upper part of

the Woodford section, whereas carbonate beds are concentrated in the lower part. These distributions are associated with the 2nd order sea level fall, with the carbonate beds the result of high stand shedding at this time scale, while the chert beds reflect increasing dissolved flux into a progressively more restricted basin.

Additional effects are introduced by geographic position within the basin. Well locations nearest the western margin had the greatest concentration of carbonate beds due to proximity to a carbonate platform. A well near the southern margin had the greatest concentration of chert, presumably the result of shedding of biogenic silica from a southern platform. A well in the basin center experienced minimal deposition of chert and carbonate; here, 3rd order sea level cycles were primarily reflected in the distribution of radiolarian-rich laminae.

2 INTRODUCTION

The characterization of stratigraphic units and surfaces in the context of sea level cycles, termed ‘sequence stratigraphy’, is now accepted as an important approach to defining correlations in depositional settings from marginal marine to the continental slope and adjacent abyssal plain. Sea level cycles function as a clock, creating recognizable and more or less regular time markers in the stratigraphic record. These markers, primarily maximum flooding surfaces and unconformities, define the maximum and minimum sea level stands. The

sequence stratigraphy approach has also been applied to lacustrine systems, where fluctuating lake levels generate correlatable units and surfaces. Here, too, water level is the clock, although the beat in lacustrine systems can be orders of magnitude faster than in marine systems.

The sequence stratigraphic approach is more problematic in fluvial and basinal settings. In fluvial settings, it is not clear that a clock exists, at least one that keeps uniform time across the entire basin. River avulsions generally do not produce a basinwide signal, and subsidence events are not necessarily synchronous across a basin, although a recent study by Fanti and Catuneaunu (2010) suggests that at least for some distance inland from the shoreline, thick coal successions correlate with marine maximum flooding surfaces. Recent investigations have focused on deciphering climate signals in the stratigraphic records of fluvial settings, but while such signals may exist, it is not clear that they are recorded in the spatial distribution of sedimentary facies or that stratigraphy provide a sufficiently distinct record.

In basinal settings of large marine basins, the problem is that the signal is weak. On a marine shelf, a 25 meter fall in sea level might represent a 25% change in water depth and an even greater shift in proximity to a shoreline. However in the middle of a basin, that same 25 meter fall in sea level might represent a 5% change in water depth and a smaller relative shift in distance to a shoreline. So it may be expected that the sea level signal be subtle.

In recent years, a number of workers have begun to test whether sequence stratigraphic approaches can apply to basinal shales. Notable among these studies are papers by Schieber (2003) and Schieber and Riciputi (2004) who argued that apparently continuous sequences of black shale in the Appalachian Basin in fact contain exposure surfaces, indicated by subtle erosion surfaces and distinct rounded pyrite grains that are interpreted as pyritized ferrous iron-rich ooids. The ooids formed during sea levels lowstands when a shale bed was exposed to shallow water, oxygenated conditions and were pyritized during the subsequent transgression. Such interpretations require that even at sea level highstands, the maximum water depth must have been relatively shallow such that the sediment-water interface was exposed to erosion during the subsequent low stands.

Our study of the Upper Devonian Woodford Shale of the Permian Basin, west Texas, was undertaken with the objective of defining criteria for recognizing stratigraphic sequences in black shales by identifying patterns in depositional facies that can be interpreted in the context of sea level changes. We report here on a study of four long cores that display a variety of rock types and sedimentary features, not just the classic laminated dark organic-rich mudstone that is sometimes assumed to be the sole constituent of black shale. The model we develop relies primarily on the stratigraphic and geographic distribution of

these non-shale lithofacies, which, we argue, are key to interpreting second and third order sea level cycles.

3 GEOLOGIC SETTING

3.1 Tectonic and Paleogeographic Setting

The Permian Basin of west Texas, or the Tobosa Basin as Comer (1991) termed its Late Devonian incarnation, formed a reentrant on the southwestern margin of the North American continent (Fig. 1). It was one of several coeval basins in North America in which organic-carbon-rich sediments were deposited, including the Oklahoma, Black Warrior, Appalachian Basin, Illinois, Michigan, Williston and Western Canada Sedimentary basins.

In the Late Devonian, the North American continent largely lay in the southern hemisphere. It was also rotated clockwise relative to its present-day position, such that the Permian Basin lay in a near-tropical setting at a paleo-latitude of approximately 20°S. All of the North American Late Devonian basins lay within a belt extending from 10° to 25°S. The global ocean lay to the south, although reconstructions by Blakey (Fig. 1) suggest that much of the western part of North America was flooded.

The Late Devonian Permian Basin was bounded to the north by exposed continental terrane of the Trans-Continental Arch, locally called the Pedernal Uplift or Massif (Fig. 2); schists and granites have been dated at 1471 and 1364 Ma (Mukhopadhyay et al., 1975). The eastern and western margins of the basin are less constrained. The eastern margin was formed by the Concho Arch; this was thought by Comer (1991) to be emergent, by Algeo et al. (2007) to be submerged, and by others (Perkins et al. 2008) to be non-existent. The western margin is more obscure. An Ordovician positive feature along present-day Rio Grande River, termed the Diablo Platform, was the site of shallow water carbonate deposition (Goldhammer et al. 1993). Comer (1991) suggested that this feature persisted through the Late Devonian. However no direct evidence of Upper Devonian in-place shallow water carbonate sediments exists, and consequently its existence must be inferred from facies relationships within the basin.

The Central Basin Platform, which during the Permian separated the Delaware Basin from the Midland Basin, did not exist in the Late Devonian; however, Ellison (1950) and Comer (1991) noted that the Upper Woodford is anomalously thin along the Central Basin Platform and the Northwest Shelf. Comer (1991) suggested that vertical movements along ancestral structures were related to tectonism at a distance along other continental margins: the Acadian Orogeny in northeastern North America and the Antler Orogeny in western North America. The eastern part of the Permian Basin was interpreted by Comer (1991) as

having been relatively shallow in the Late Devonian, as were the Northwestern and Eastern Shelfs. He noted that the thickest, most complete Woodford sections were found in the areas of the Delaware and Val Verde Basins, suggesting that these areas were the deepest parts of the Late Devonian Permian Basin.

3.2 **Silurian through Mississippian Stratigraphy**

The Woodford Shale is part of a Paleozoic succession dominated by carbonate and shale successions (Figure 3). It overlies the Lower to Middle Devonian Thirtyone Formation in the Delaware Basin and coeval Devonian Limestone in the Midland Basin and on the Central Basin Platform, separated by a regional unconformity that elsewhere in the Midcontinent removed older Devonian and some Silurian strata. Comer (1991) reported that 'cavernous limestone' underlies black shale in a well from Lea County, New Mexico, suggesting that this unconformity was at least locally accompanied by prolonged exposure and karst development.

The Woodford is unconformably overlain by the Rancheria Formation in the Delaware Basin and the Mississippian Limestone in the Midland Basin and on the Central Basin Platform. In the Delaware Basin, the time interval represented by the unconformity includes the Kinderhookian, Osagean and part of the Meramecian stages, a period of approximately 20 million years.

Comer (1991) reports dates of latest Givetian to earliest Mississippian for the Woodford. A subsequent conodont study, sampling wells in the Midland Basin (eastern Permian Basin) (Meyer and Barrick, 2000) restricted the age of organic-rich shale somewhat; they described a 'pre-Woodford' green and grey shale with latest Givetian and Frasnian conodonts and a typical Woodford, organic-rich black shale with middle to late Fammennian conodonts.

3.3 **Woodford Stratigraphy and Regional Correlations**

Ellison (1950) and subsequently Comer (1991) recognized that the Woodford can be divided into three members, based on gamma log response. These members are correlative regionally across the basin; our work here is consistent with this previously developed stratigraphy. The members include a Lower Woodford member with relatively low gamma ray, a Middle Woodford member with remarkably high gamma ray, and an Upper Woodford member with relatively low gamma ray. Even the lower gamma ray signatures of the Lower and Upper members are high in the context of most shales; both units commonly has gamma ray readings of 100 to 200 API units, but gamma ray readings in the Middle Woodford are typically 300 to 500.

The Woodford in the Permian Basin is correlative with the upper part of the Caballos Novaculite in the Marathon region of west Texas, the Percha Formation

in Hueco and Franklin Mountains of west Texas, and the Sly Gap Formation of southeastern New Mexico. The Percha is a black, fissile, non-fossiliferous shale, whereas the Sly Gap Formation is a fossiliferous tan to pale yellow shale, siltstone and limestone (Comer 1991).

3.4 **Dataset and Methods**

Our data come from long cores in four wells in west Texas: the Reliance Triple Crown (RTC) #1 well (290 feet; 88.4 m) and the La Escalera B55 well (174 feet; 53.0 m) in western Pecos County, the Keystone Cattle Company (KCC) 503 well in Winkler County (303.5 feet; 92.5 m), and the MBF well (250 feet; 76 m) in Reeves County. These cores represent 78%, 61% and 52% of the total Woodford thickness at the locations of the first three wells; we were not provided logs for the MBF well and do not know the thickness of the complete Woodford section at this location.

The cores were initially described in detail at a scale of 1:16; condensed versions of the descriptions shown in Figures 4 to 7. Original descriptions included: identification of lithologies, sedimentary structures including both physical lamination and bioturbation, the presence of cements including calcite, dolomite and pyrite, and the presence, intensity and orientation of fractures relative to vertical. The RTC #1 and KCC 503 cores were sampled for petrographic thin sections; these were found invaluable for corroborating lithologic identification,

documenting bedding styles in very fine-grained rocks, and identifying microfossils. Additional samples were taken for geochemical analysis (Mnich 2009).

Cores were correlated to electric logs provided to us by the well operators: Pioneer Natural Resources (RTC #1 well); Petro-Hunt (B55 well); and Whiting Petroleum (KCC 503 well). These logs included both wireline and core gamma logs, which were invaluable in correlating cores to logs.

Radiometric age dates were obtained on four samples from the RTC#1 core using the Re-Os method. Samples were selected to obtain a wide stratigraphic range and picked to avoid any evidence of hydrothermal alteration (filled fractures or veins).

4.0 **RESULTS**

4.1 **Lithofacies**

Five lithofacies are present throughout most of the Woodford: mudstone, mudstone with phosphate nodules, dolomite, bedded chert, radiolarian-carbonate laminae, bioturbated mudstone and massive chert (novaculite).

4.1.1 Mudstone

Mudstone is the overwhelmingly dominant lithology in the Woodford, amounting from 85 to 99% of the formation in all wells (Figures 4 to 7). This rock is composed predominantly of quartz and clays in proportions from 1.5:1 to 8:1, with quartz content increasing upward through much of the formation (Mnich, 2009; Harris et al., 2009). Total organic carbon (TOC) content ranges from 1 to 14 weight % and, based on the gamma ray log that is highly correlative with TOC, appears to be cyclically distributed. Dolomite is a significant component of mudstone only near the base of the formation. Minor components of the shale include pyrite and feldspar. The mudstone is not notably fossiliferous. Tasmanites cysts are dispersed throughout (Fig. 10E), as are recrystallized radiolarian. We have tentatively identified agglutinated foraminifera.

The mudstone is variably laminated, in places displaying a distinct submillimeter-scale parallel lamination (Figs. 8A, 10A), but elsewhere faintly bedded or massive (Fig. 8B). Discerning lamination is surprisingly difficult, even when digital photos have been processed to enhance features and even in thin section. Considerable effort was devoted to resolving whether the massive nature was real, and if so, whether it was a primary physical depositional fabric or resulted from bioturbation.

Laminae in the finely laminated mudstones displays subtle pinching and swelling at a scale of 2-4 cm, although truncations of laminae were not noted. Laminae

also display disruptions, suggesting a bioturbated fabric, although definitive burrow structures were not identified. Massive mudstones lack vertical changes in grain size or composition, but nonetheless have a planar fabric defined by the orientation of organic particles such as flatten Tasmanites cysts, foraminfera or clay.

Disturbed or convolute bedding, interpreted as soft sediment deformation, is relatively rare. One 10 foot thick (3 meter) section from the La Escalera core contains discordant bedding and locally flow folds; we have interpreted this as a large slumped interval..

Two additional sedimentary features are common. One is a flared structure of white carbonate (Fig. 8C), associated with a thin brittle layer, typically 2 to 3 cm in height and 4 cm in diameters. We assume that they are conical in form but were not able to see them in plan view. We interpret these as fluid escape structures, either gas or water. A second structure consists of thin highly convoluted sheets (Fig. 8D), commonly 2 cm in height; in plan view, they are linear and at least a few cm long. These are interpreted as synerisis cracks, nearly syndepositional features that were originally planar but became convoluted during compaction. It is common to see multiple such features restricted to a single bed that presumably a fair degree of cohesiveness just after deposition.

4.1.2 Dolomite

Dolomite is found in discrete beds from 1 to 30 cm thick, commonly in the range of 2 to 8 cm (Figs. 9A, 10B). Dolomite is micritic to silt-size in these beds, locally exhibiting subtle grading in the uppermost one to two millimeters. Recognizable bioclasts are virtually never present; one bryazoan fragment was found. The thickest of the beds, in the lower part of the section in the RTC #1 well, contained several dark mudstone clasts, identical to the mudstones. One bed is composed of what appear to be fragments of laminated dolomite; we interpret these a broken and redeposted fragments of a dolomite crust. Beds are largely massive but rarely show parallel lamination in the thickest beds.

4.1.3 Bedded Chert

Chert occurs in beds generally 3 to 10 cm thick (Fig. 9C). The chert is extremely hard, dark (in fact similar in color to and sometimes difficult to distinguish from the mudstone) and contains internal vertical fractures. It is composed of radiolaria that are variously recrystallized and small amounts of clay and carbonates. The chert is massive to laminated on a scale less than 1 mm and may show grading from 100% upward into fine grain material, typically fine quartz, clay and organic matter.

4.1.4 Radiolarian laminae

Radiolaria are concentrated in laminae 2 mm or less in thickness (fig. 8F and 10C) that also contain fine grained material, including quartz, organic matter and clay. Coarse carbonate, probably dolomite is commonly present in these laminae, which we interpret as a diagenetic product. These laminae are sharp-based and may have sharp or gradational tops.

4.1.5 Mudstone with phosphatic nodules

The mudstone locally contains numerous phosphatic concretions (Fig. 8E) in two narrowly defined stratigraphic intervals, one in the Upper Woodford in the RTC #1 and MBF cores a few meters above the gamma log break defining the Middle Woodford – Upper Woodford boundary (Figs. 4 and 6), comprising approximately 10% of the section. One additional interval of phosphatic concretions was noted, a 1.5 meter thick section in the Lower Woodford section of the La Escalera core. These concretions are irregularly flattened parallel to bedding, generally 3 to 5 cm in thickness and 5 to 10 cm in length. They consist of apatite and quartz (chert), in which apatite crystals form euhedral crystals in a groundmass of microcrystalline quartz (Fig. 10D).

4.1.6 Massive chert (novaculite)

Two types of chert are present near the top of the section: a white and a dark grey chert (Figs. 6 and 9D). These are enriched in quartz relative to the underlying and overlying mudstones, as reported by Chesapeake from XRD analysis (78% in one sample), with minor illite/smectite (17%), feldspar (5%) and pyrite (1%). We lack the data to account for color differences between the two types of chert.

This unit may be a tongue of the Caballos Novaculite, the top of which is dated in the Marathon Basin at upper Frasnian or lowermost Kinderhookian (Noble, 1992).

4.1.7 Bioturbated mudstone

The dark, organic carbon-rich mudstone is sharply overlain by a lighter grey, pervasively bioturbated mudstone in the MBF well (Figs. 6 and 9E). Sedimentary structures are rarely visible in this interval (bioturbation index of grade 5 or 6, following the classification of Taylor and Goldring, 1993); the rare preserved structures are thin wavy laminae. The burrowing appears to be dominated by simple small burrows, although textures were indistinct. Possible rare large Teichicnus burrows were found, suggesting fully oxygenated conditions in mid- to outer shelf water depths.

Mineralogical composition of the bioturbated mudstone is similar to the underlying organic-rich mudstone. Quantitative XRD reports from Chesapeake indicate compositions dominated by quartz (average of 4 samples was 61%) and illite/smectite (23%) with subordinate feldspar (8%) and dolomite (3%). Total organic carbon contents in this facies are greatly reduced in comparison with the underlying dark mudstone. TOC data provided by Chesapeake averaged 0.86% in this interval (Fig. 6).

4.2 **Geographic distribution of lithofacies**

The distribution of lithofacies varies substantially between the four wells studies here. Two key points include:

(1) Carbonate beds are most common in the western wells, the MBF (60 individual beds) and RTC #1 wells (38 beds). Moreover, the upper part of the Upper Woodford was truncated by erosion in the RTC #1 well, so the pre-erosion section might have contained more carbonate. Only 17 beds were identified in the La Escalera core and 6 were identified in the long KCC #1 core (although this core is similar in length to the RTC#1 core, it covers a shorter stratigraphic interval because the Woodford section expends in the basin center.

(2) Chert beds are most common in the southernmost well, the Petro-Hunt La Escalera well (166 beds). They are less common in the RTC #1 well (16 beds) and relatively rare in the two northernmost wells, the KCC 503 and MBF (5 beds in each).

Bioturbated mudstone and novaculite are present only in the Chesapeake MBF core may not be significant. However, the upper part of the Upper Woodford section was truncated by erosion in the RTC #1 well, removing the equivalent section, and this part was not cored in the KCC 503 and La Escalera wells.

4.3 Vertical distribution of facies

The distribution of facies is shown in Figures 3 through 6. Most of the formation is organic mudstone with interspersed chert and dolomite beds and radiolarian laminae. This organic-rich section is overlain by, in succession, mudstone with phosphate nodules, an additional interval of organic-rich mudstone, chert (novaculite) and bioturbated organic-poor mudstone.

Within the overall succession are some distinctive patterns to the distribution of carbonate and chert beds within the organic-rich mudstone. Chert beds are generally concentrated in the upper part of the formation. This is particularly the case in RTC #1 core (Fig. 4), where the lowermost chert beds occur just below the Middle Woodford – Upper Woodford contact and are common up to the top of

the core. In the KCC 503 well (Fig. 5), chert beds are clustered around the high TOC / high gamma ray spike near the Middle Woodford Upper Woodford contact. In the La Escalera core (Fig. 7), where chert beds are most abundant and are present throughout the entire core, there is still a greater concentration in the upper part of the section.

The stratigraphic distribution of carbonate beds varies between wells. In MBF well, carbonate beds are most abundant in the middle of the section and immediately below the transition to novaculite (Fig. 6). As noted above, we lack electric logs for this well and cannot place the data exactly with respect to the Lower, Middle and Upper Woodford units. In the RTC #1 well, carbonate is clearly preferentially distributed in the lower part of the section (Fig. 4), a distribution approximately antithetic to the chert.

A cyclic distribution of carbonate beds is evident in the RTC #1 core (Fig. 4). The carbonate beds occur in bundles, intervals in which their occurrence is common, separated by intervals in which no carbonate is present. At least 10 such cycles are evident in the RTC #1 core, ranging in thickness from 6 meters (19 feet) to 14 meters (46 feet). There are no obvious patterns to the vertical distribution of cycle thickness or to the relative proportions of sections with and without carbonate beds. The thickest beds are found near the base of the section, but the thickness of the beds does not obviously vary within cycles.

A cyclicity is also evident in the radiolarian laminae in the KCC 503 core (Fig. 5). These laminae also occur in bundles, concentrated in some intervals with densities of 2.5 / meter, while intervening intervals have from 0 to 1 / meter. In the 93 meters of cored section in this well, 3.5 cycles are present, so each cycle averages 26.5 meters. However, the overall Woodford section has expanded by approximately 200%, so the relative thickness of each cycle is approximately similar between the two wells.

Our data from the RTC #1 and KCC 503 wells (Figs. 4 and 5) suggest that the radiolarian bundles and dolomite bundles are antithetically organized, that the dolomite beds are concentrated where the radiolarian laminae are sparse and vice versa. That is clearly the case in the KCC 503 well, where dolomite beds are uncommon. This organization is less clearly in the RTC #1 but is nonetheless a plausible interpretation.

4.4 Age dates

The lowermost sample, from the Lower Woodford, was dated at 379.0 ± 7.9 Ma (middle Frasnian) (Fig. 4). Samples from the lower and upper parts of the Middle Woodford were dated at 371.5 ± 5.8 Ma and 364.0 ± 13 Ma, respectively (spanning the Fammennian). The uppermost sample, from the Upper Woodford, was dated at 357.9 ± 5.3 Ma (Tournaisian – lowermost Mississippian).

Sedimentation rates calculated from these dates yields a best estimate of 4.04 meters of sediment (compacted) deposited per million years for the RTC #1 section, with a range of possible sedimentation rates based on the uncertainty in individual ages of 3.03 to 5.40 meters per million years. Sedimentation rates appear to have been remarkably constant through time.

5 DISCUSSION

5.1 Depositional Processes

Three primary mechanisms exist for transport of mud into basinal settings: pelagic fallout of suspended material, traction deposits or sediment gravity flows of different types. The latter may include mass flow deposits, true turbidites and the recently described wave-enhanced sediment gravity flows (Macquaker et al., 2010). The latter describes beds with a lower silt or very fine-grained sand layer with ripple laminae, a middle layer of silt and clay with wavy parallel lamination and a draping upper layer of silt and clay. Traction deposits consist of ripple cross-laminated muds; these have been produced in flume experiments (Schieber and Southard, 2009) and observed in the rock record (Schieber and Yawar, 2009). Identification of such ripple structures in core can be difficult because the low initial amplitude of the structures and the high degree of compaction in mudstones.

Woodford mudstones range from finely laminated to poorly laminated to massive. Even the finely laminated mudstones exhibit ‘ragged’ lamination. We suggest that suggest that components of mudstone were introduced to the deep basin through different processes. Fine grained carbonate originated on basin margin platforms and was transported to the basin as sediment gravity flows. Clays were introduced from the Pedernal Massif to the north; it probably accumulated initially on a shallow water shelf and was then transported and redeposited in the deep basin by mud flows and turbidity currents. Other components, specifically organic matter and radiolarian, formed in the water column and sank to the bottom as pelagic rain, possibly as floccules (Macquaker et al., 2010). Pinching and swelling of laminae suggests that sediments were reworked by bottom currents. Modification by bioturbation is likely, although we it is difficult to identify discrete burrow structures.

Interpretation of the non-mudstone facies is more straightforward The dolomite beds have many characteristics of classic turbidite beds: they are largely massive, with sharp bases and subtle grading at the top to finer sediments. A few beds exhibit parallel lamination. The thickest dolomite bed contains rip-up clasts of black mudstone, indicating that it was incorporated into a turbidity current with sufficient energy to scour the underlying muddy substrate.

The radiolarian laminae are also probably turbidite deposits, although this interpretation is less definitive than that of the dolomite beds.

The chert beds can also be interpreted as turbidites. They have sharp bases, commonly show an upward decrease in radiolarian spherules and an upward increase in the content of fine-grained material (clay and organic matter) and are planar laminated. Radiolarian chert beds that originated as turbidites are described elsewhere, for example Swarbrick (1967) and Sedlock and Isozaki (1990). This model implies that radiolaria must have locally accumulated in shallower water as uncemented sediment and were then transported under the influence of gravity and redeposited in basinal settings. One other possible origin should be considered, however. These may have originated as a pelagic rain-out of radiolaria from the water column. The great abundance would have been the result of a nutrient slug to the basin, and the grading upward to a normal mudstone the result of depletion of the water column.

5.2 Sea Level

5.2.1 Second order sea level cycle

The stratigraphic progression of Woodford lithofacies is from organic-rich mudstone with no bioturbation (or possibly local cryptobioturbation) upward to heavily bioturbated organic-poor mudstone with an infauna characteristic of mid-shelf depths. This suggests that water depths decreased significantly during deposition of the Woodford. This interpretation is consistent with organic

petrology data from the RTC #1 well, which shows a distinct increase in the fraction of terrestrial kerogen in the Upper Woodford (Mnich, 2009).

Physical sedimentary structures are consistent with this interpretation. In the organic-rich mudstones, coarse sediment was introduced only through the action of sediment gravity flows; there is no indication of persistent traction currents. In the bioturbated mudstone at the top of the Woodford section, remnants of wavy bedding are preserved that are consistent with an interpretation of fair-weather or storm wave influence, in other words inner to mid shelf depths.

Decreasing water depths could have resulted either (1) a fall in eustatic sea level, (2) sedimentation outpacing subsidence, or (3) tectonism. In this case, we and others see little evidence for orogenic uplift, so it is unlikely that there was a tectonic component to basin shallowing. Eustacy, however, could have been a significant contributor to shallowing. Haq and Schutter (2008) describe a 2nd order sea level fall of approximately 70 meters from the earliest Frasnian to the latest Famennian. Moreover, two extreme 3rd order sea level falls occurred within the Tournaisian, one at the Famennian-Tournaisian boundary and a second approximately 6 m.y. later. Both were on the order of 100 meters, superimposed on the 70 meter 2nd order fall. So a total sea level fall of 170 meters is possible, based solely on eustacy.

Within the basin, 90 to 200 meters of shale were deposited over a period of approximately 20 million years. Assuming Airy isotocy, then crustal subsidence due to sedimentation alone would have amounted to X meters during this time; thus the basin would have shallowed by XXX meters. The combined effect of eustatic sea level fall and sedimentation would have been a decrease in sea level of XX meters.

If we assume, fairly arbitrarily, a water depth of 50 meters for deposition of the bioturbated mudstone, that would place water depth at the start of organic mudstone deposition at approximately XX.

5.1.2 Third order sea level cycles

The distinctive bundling of carbonate beds in the RTC #1 core can be interpreted as a productive of high stand shedding. This process is associated with carbonate platforms and has been described in many Quaternary platforms and is manifested in maximal transport of shallow water carbonate to the adjacent deep basin during sea level high stands (Schlager et al., 1994). It depends on three relationships: (1) carbonate production is greatest during highstands when large areas of the platform are shallowly submerged, yet accommodation space is minimal; (2) carbonate production decreases during transgressions when the platform is deeply submerged, at the same time when accommodation space

increases; (3) carbonate production is also low during low stands when carbonate platforms are exposed.

The bundles of dolomite beds therefore indicate sea level high stands. We identify at least 10 of these in the RTC #1 core (Figure XX); more may be present if these can be subdivided. This number is broadly consistent with 16 3rd order eustatic cycles between the 2nd order sea level high stand in the earliest Frasnian to the 2nd order low stand at the Devonian – Mississippian boundary (Haq and Schutter, 2008). In general, sea level oscillations during the Frasnian are relatively muted in amplitude, typically 30 meters; the amplitude is 50 to 60 meters during the Famennian.

If the intervals with abundant dolomite beds represent sea level high stand systems tracts, then the intervening sections without dolomite beds represent the low stand and transgressive systems tracts, and the sequence boundary boundary should be placed at or just above the uppermost dolomite bed in each bundle. We see no obvious change in continuous mudstone section that might represent either the sequence boundary or the transition between low stand and transgressive systems tracts. We surmise that the bulk of that interval is represented by the transgressive systems tract.

Our data from the RTC #1 core suggest that the radiolarian laminae are concentrated in intervals in which the carbonate beds are absent, although the

relationship is not clear cut. We offer a possible explanation for this. Radiolarian may proliferate during low stands and in the early part of transgressions because dissolved silica may be more concentrated in the water column than during high stands (Mnich, 2009). The bulk of the dissolved silica must be derived from chemical weathering of the continental terrane north of the basin. During low stands, more continental terrane is exposed, so the flux of dissolved silica to the basin should be greater. Moreover, the volume of water in the basin is less during the low stands, with the combined effect being a substantial increase in silica concentration.

The Woodford data allow us to test common models for interpreting stratigraphic sequences and for organic carbon enrichment. High gamma ray values are commonly used as a basis for identify transgressive systems tracts and maximum flooding surfaces. This relationship could be due to (1) high clay content during transgressions, as the deposition of coarse clastics shifts landward, or (2) a model that organic carbon deposition increases during transgressions, perhaps the result of lack of dilution by clastics. Figure 11 displays the gamma ray log and our TOC data in relationship to our inferred 3rd order sea level cycles in the RTC #1 core. In this case, high gamma ray values are associated with high uranium content, not high clay content, based on spectral core gamma logs; in fact the contribution of potassium to the total gamma ray log is fairly small. The data in Figure 11 shows that in the lower half of the Woodford, in fact the highest gamma ray and TOC values correspond to

the carbonate bundles – in other words the high stand systems tracts, whereas TOC values are lower in the low stand and transgressive systems tracts. That relationship reverses in the upper half of the Woodford, where TOC values are highest during the lowstand and/or transgressive systems tracts. That the relationship changes suggests a basic change in the mechanism of organic carbon accumulation.

5.2.3 Distribution of carbonate and chert beds

In the RTC #1 well, carbonates are largely restricted from that point to the bottom of the formation. We suggest that the same mechanisms described above for 3rd order cycles also apply to these beds at a 2nd order scale. Sea level was near a 2nd order high stand during the Frasnian, so that when 3rd order high stands occurred, the platform was highly productive and significant volumes of carbonate were shed to the adjacent basin. In the Famennian, however, as the 2nd order low stand was approached, even during high stands the platform may have been partially exposed, thus minimizing carbonate production and shedding.

Chert beds may also be governed by the same processes at 2nd and 3rd order scales. Chert beds in the RTC #1 well occur from the upper part of the Middle Woodford to the top of the formation but are not found below. Similar relationships are present in the La Escalera core. Dissolved silica concentrations

would have been generally lower during the Frasnian 2nd order high stand, so radiolarian productivity could have been less. During the 2nd order sea level fall to the Devonian-Mississippian boundary, silica concentrations should have increased. Moreover, if the chert beds are detrital in origin, with siliceous sediment transported as turbidites, then the 2nd order sea level fall could have forced migration of the source area toward the basin center.

In the KCC 503 core, the five chert beds are clustered around a high TOC spike at the top of the Middle Woodford. This suggests that organic productivity and nutrient delivery were also factors in the distribution of chert beds.

5.3 Paleogeographic controls

Location within the basin also clearly played a substantial role in the stratigraphic record. Significant differences in lithofacies exist between the wells: (1) Chert beds are abundant in the La Escalera well throughout the core, but are present only in the upper part of the section in RTC #1 and are rare in the KCC 503 core. This suggests a southern source for the radiolaria. (2) Carbonate beds are abundant in the MBF cores and abundant in the lower and middle Woodford sections in the RTC #1 core. They are rare in the other cores. These relationships suggest that a carbonate platform existed to west of the Permian Basin, as suggested by Comer (1991), and that only the proximal wells (MBF and

652 RTC #1) were close enough to the proposal to receive much carbonate
653 sediment.
654
655 5.4 **Other criteria for recognizing stratigraphic sequences**
656
657 No evidence for exposure surfaces exists in the Woodford cores. We are aware
658 that truncations in mudstone formations may display very low angles (Schieber,
659 2003) and can therefore be difficult to recognize in core but nonetheless found no
660 such features in either hand specimen or thin section examination. We also
661 found no features resembling the pyritized chamositic ooids described by
662 Schieber and Riciputi (2004), which they associate with erosional surfaces and
663 interpret to have formed originally as iron clay ooids in an oxygenated water
664 column. The absence of these features suggests that water depths during
665 deposition of the much of the Woodford section were great enough so that the
666 sediment was never subaerially exposed.
667
668 6 **CONCLUSIONS**
669
670 The Woodford Shale exhibit a number of sedimentological and stratigraphic
671 features that, when integrated, can be used to formulate a 2nd and 3rd order
672 sequence stratigraphic framework. Features indicative of a 2nd order sea level
673 fall are (1) a transition upward from organic-rich non-bioturbated or crypto-
674 bioturbated mudstone to organic-poor highly bioturbated mudstone, (2) a change

upward from amorphous, algal-derived organic matter to terrestrial organic matter, (3) phosphate nodules near the top of the organic-rich mudstone, and (4) increased frequency of chert beds and decreased frequency of carbonate beds in the upper part of the section. In part these are depositional effects, related to the changing balance between carbonate production and accommodation space (beds of allochthonous carbonate). In part these are related to oxygen levels in the paleowater column, which impacts the viability of a vigorous infauna (degree of bioturbation) and early diagenetic reactions in the sediment (phosphate precipitation). Finally, we suggest that the changing balance between chemical runoff, specifically dissolved silica, and the size of the water mass in the basin results in enhanced chert formation.

Third order sea level cycles are revealed by cyclicity in non-mudstone facies, specifically beds of allochthonous carbonate, deposited as turbidites, and radiolarian-rich laminae, which probably also represent deposition from sediment gravity flows. Carbonate beds interbedded with organic-rich mudstone represent the highstand systems tract; we invoke a model of high stand shedding to account for the carbonate. The sequence boundary is placed at or just above a transition to continuous organic mudstone, which in turn represent the low stand and transgressive systems tracts. These 3rd order cycles are typically 5 to 12 meters thick. Taken together, the Woodford represent the falling sea level half of a 2nd order cycle and at least 10 complete 3rd order cycles.

We suggest that two features classically associated with stratigraphic sequences, either high gamma ray values due to concentrations of clay or organic matter indicating flooding surfaces, or exposure surfaces indicating sequence boundaries, are absent from the stratigraphic record in the Woodford Shale. While a cyclic pattern of high gamma ray values is present, it reflects high TOC and not high clay content; moreover, the high TOC in parts of the section is associated with high stands and not transgressions. Nor do we see evidence for exposure surfaces or systematic occurrence of shallow water deposition until the top of the section.

7 REFERENCES

Algeo, T.J., Lyons, T.W., Blakey, R.C., and Over, D.J., 2007, Hydrographic conditions of the Devono-Carboniferous North American Seaway inferred from sedimentary Mo-TOC relationships: Palaeogeography, Palaeoclimatology, Palaeoecology, v. 256, p. 204-230.

Comer, J.B., 1991, Stratigraphic analysis of the Upper Devonian Woodford Formation, Permian Basin, west Texas and southeastern New Mexico: Texas Bureau of Economic Geology Report of Investigations No. 201, 63 pp.

719 Ellison, S.P., Jr., 1950, Subsurface Woodford black shale, west Texas and
720 southeast New Mexico: Bureau of Economic Geology, Report of Investigations,
721 No. 7, 20 p.
722
723 "Permian Basin." *Encyclopædia Britannica. Encyclopædia Britannica Online Academic*
724 *Edition*. Encyclopædia Britannica Inc., 2012. Web. 27 Feb. 2012.
725
726 Fanti, F. and Catuneanu, O., 2010, Fluvial sequence stratigraphy; the Wapiti
727 Formation, west-central Alberta, Canada: Journal of Sedimentary Research, v.
728 80, p. 320-338.
729
730 Goldhammer, R.K., Lehmann, P.J., and Dunn, P.A., 1993, The origin of high-
731 frequency platform carbonate cycles and third-order sequences (Lower
732 Ordovician El Paso Gp, west Texas): Constraints from outcrop data and
733 stratigraphic modeling: Journal of Sedimentary Petrology, v. 63, p. 318-359.
734
735 Haq, B.U., and Schutter, S.R., 2008, A chronology of Paleozoic sea-level
736 changes: Sciences, v. 322, no. 5898, p. 64-68.
737
738 Harris, N.B., Hemmesch, N.T., Mnich, C.A., Aoudia, K., and Miskimins, J., 2009,
739 An integrated geological and petrophysical study of a shale gas play: Woodford
740 Shale, Permian Basin, west Texas: Gulf Coast Associations of Geological
741 Societies, Transactions, v. 59, p. 337-346.

Macquaker, J.H.S., Bentley, S.J., and Bohacs, K.M., 2010, Wave-enhanced sediment-gravity flows and mud dispersal across continental shelves: Reappraising sediment transport processes operating in ancient mudstone successions: Geology, v. 38, p. 947-950.

Macquaker, J.H.S., Keller, M.A., and Davies, S.J., 2010, Algal blooms and "marine snow": mechanisms that enhance preservation of organic carbon in ancient fine-grained sediments: Journal of Sedimentary Research, v. 80, p. 934-942.

Meyer, B.D., and Barrick, J.E., 2000, Conodonts from the Woodford Formation (Late Devonian) and adjacent units, subsurface west Texas and eastern New Mexico, *in* DeMis, W. D., Nelis, M. K., and Trentham, R. C. (eds.), The Permian Basin: Proving ground for tomorrow's technologies: West Texas Geological Society, Publication 00-109, p. 229-237.

Mnich, C.A., 2009, Geochemical signatures of stratigraphic sequences and sea-level change in the Woodford Shale, Permian Basin [M.Sc. thesis]: Golden , Colorado School of Mines, 89 p.

763 Mukhopadhyay, B., Brookins, D.G., and Bolivar, S.L., 1975, Rb-Sr whole-rock
764 study of the Precambrian rocks of the Pedernal Hills, New Mexico: Earth and
765 Planetary Science Letters, v. 27, p. 283-286.
766
767 Noble, P., 1992, Biostratigraphy of the Caballos Novaculite – Tesnus Formation
768 boundary, Marathon Basin, Texas: Palaeogeography, Palaeoclimatology,
769 Palaeoecology, v. 96, p. 141-153.
770
771 Perkins, R.B., Piper, D.Z., and Mason, C.E., 2008, Trace-element budgets in the
772 Ohio/Sunbury shales of Kentucky: Constraints on ocean circulation and primary
773 productivity in the Devonian-Mississippian Appalachian Basin:
774 Palaeogeography, Palaeoclimatology, Palaeoecology, v. 265, p. 14-29.
775
776 Schieber, J., 2003, Simple gifts and buried treasures – Implications of finding
777 bioturbation and erosion surfaces in black shales: The Sedimentary Record, v.
778 1, p. 4-8.
779
780 Schieber, J., and Riciputi, L., 2004, Pyrite ooids in Devonian black shales record
781 intermittent sea-level drop and shallow-water conditions: Geology, v. 32, p. 305–
782 308.
783

784 Schieber, J., and Southard, J.B., 2009, Bedload transport of mud by floccules
785 ripples – Direct observation of ripple migration processes and their implications:
786 Geology, v. 37, p. 483-486.
787
788 Schieber, J., and Yawar, Z., 2009, A new twist on mud deposition – Mud ripples
789 in experiment and rock record: The Sedimentary Record, v. 7, p. 4-8.
790
791 Schlager, W., Reijmer, J.J.G., and Droxler, A., 1994, Highstand shedding of
792 carbonate platforms: Journal of Sedimentary Research, v. B64, p. 270-281.
793
794 Sedlock, R.L., and Isozaki,Y., 1990, Lithology and biostratigraphy of Franciscan-
795 like cherts and associated rocks in west-central Baja California, Mexico:
796 Geological Society of America, v. 102, p. 852-864.
797
798 Swarbrick, E.E., 1967, Turbidite cherts from northeast Devon: Sedimentary
799 Geology, v. 1, p. 145-157.
800
801 Taylor, A.M., and Goldring, R., 1993, Description and analysis of bioturbation and
802 ichnofabric: Journal of the Geological Society, London, v. 150, p. 141-148.
803

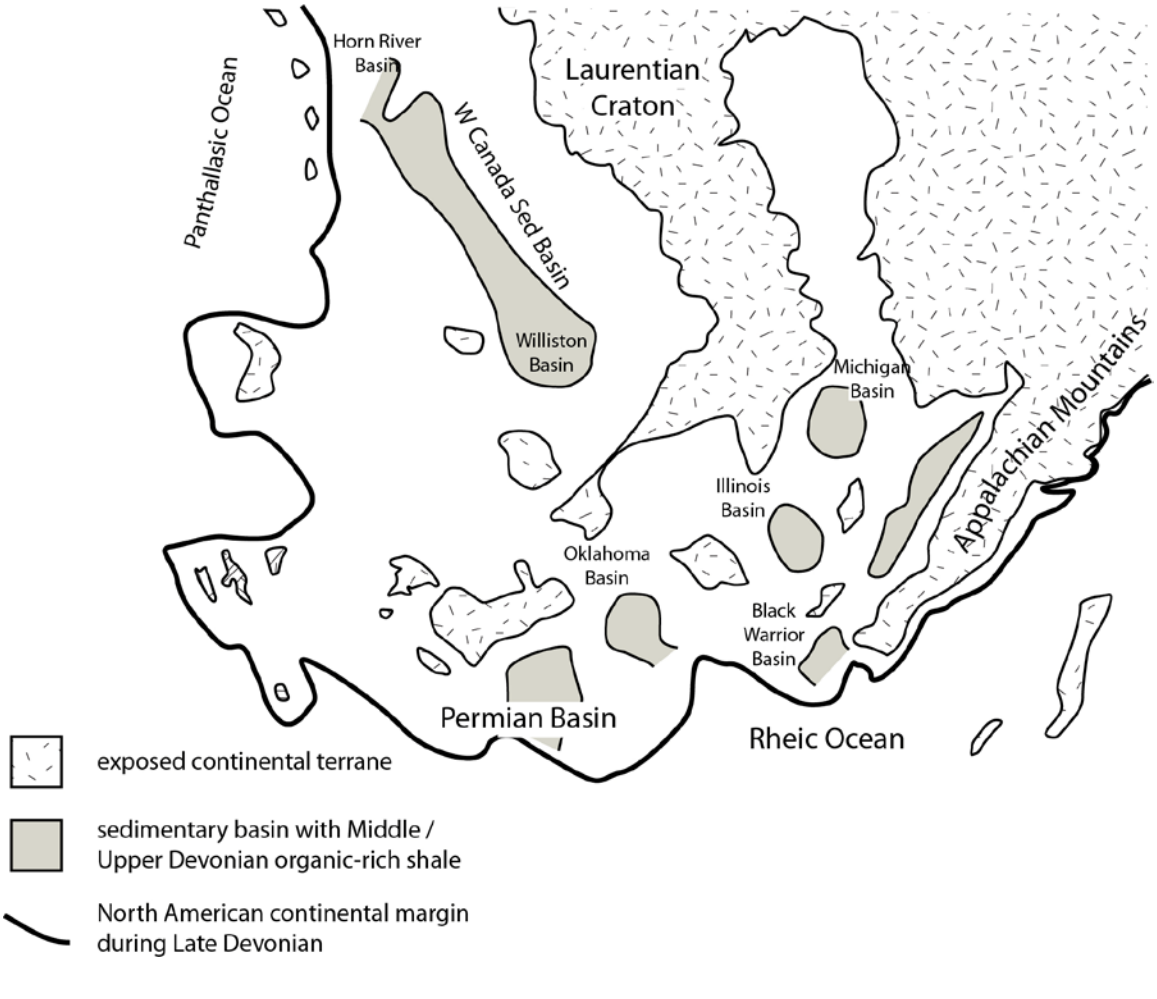

Figure 1. Map of the North American continent in Late Devonian. Modified after Algeo et al. (2007).

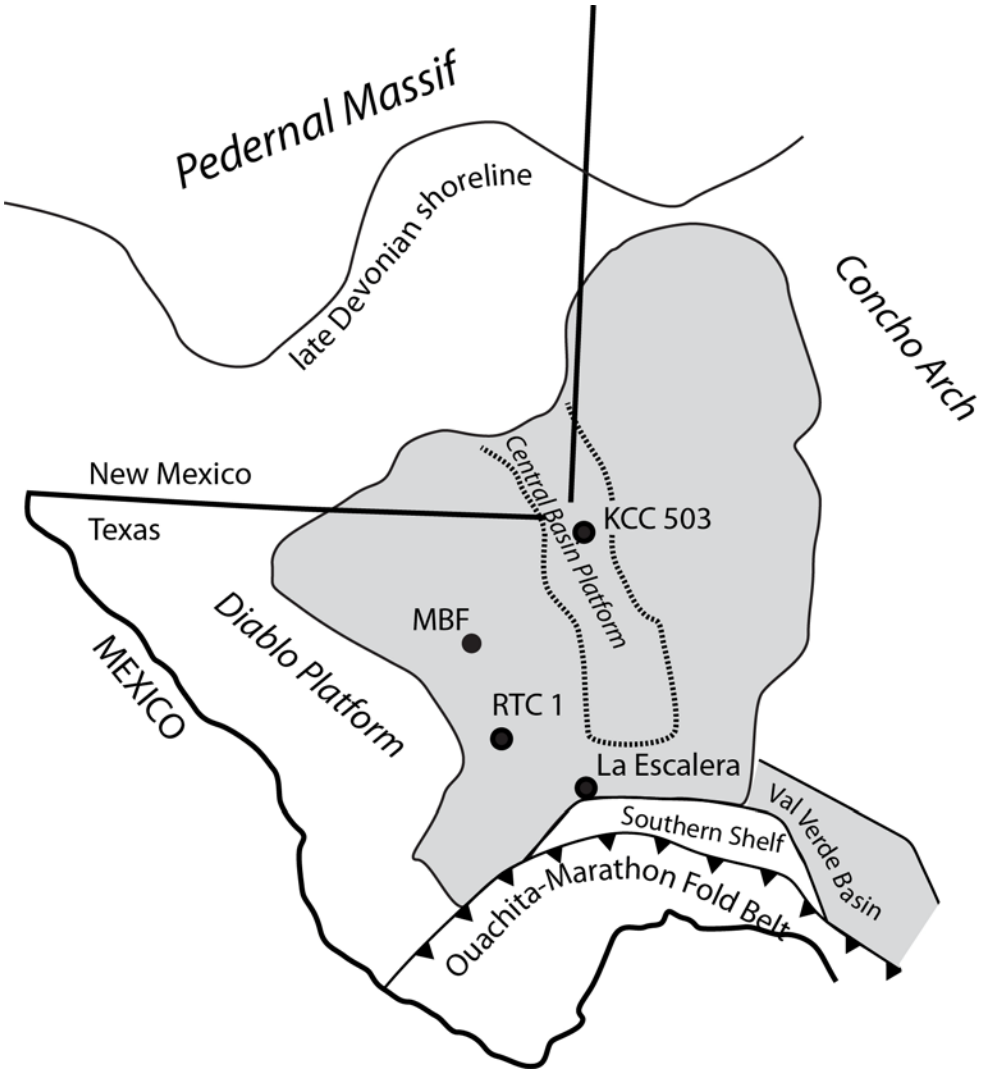

Figure 2. Map of the Permian Basin, showing locations of well included in the study and key paleogeographic features.

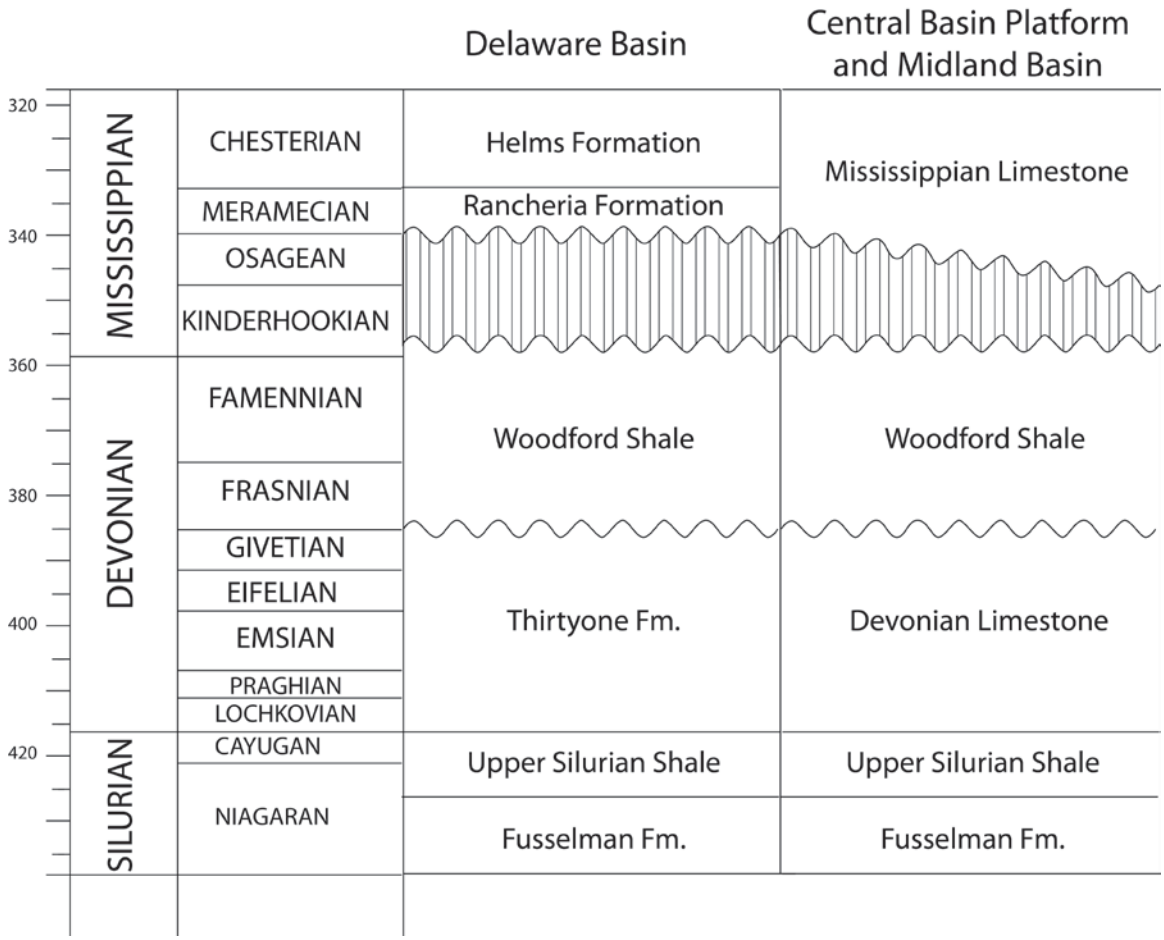

Figure 3. Silurian through Mississippian stratigraphy of the Permian Basin. Modified after Comer (1991) and

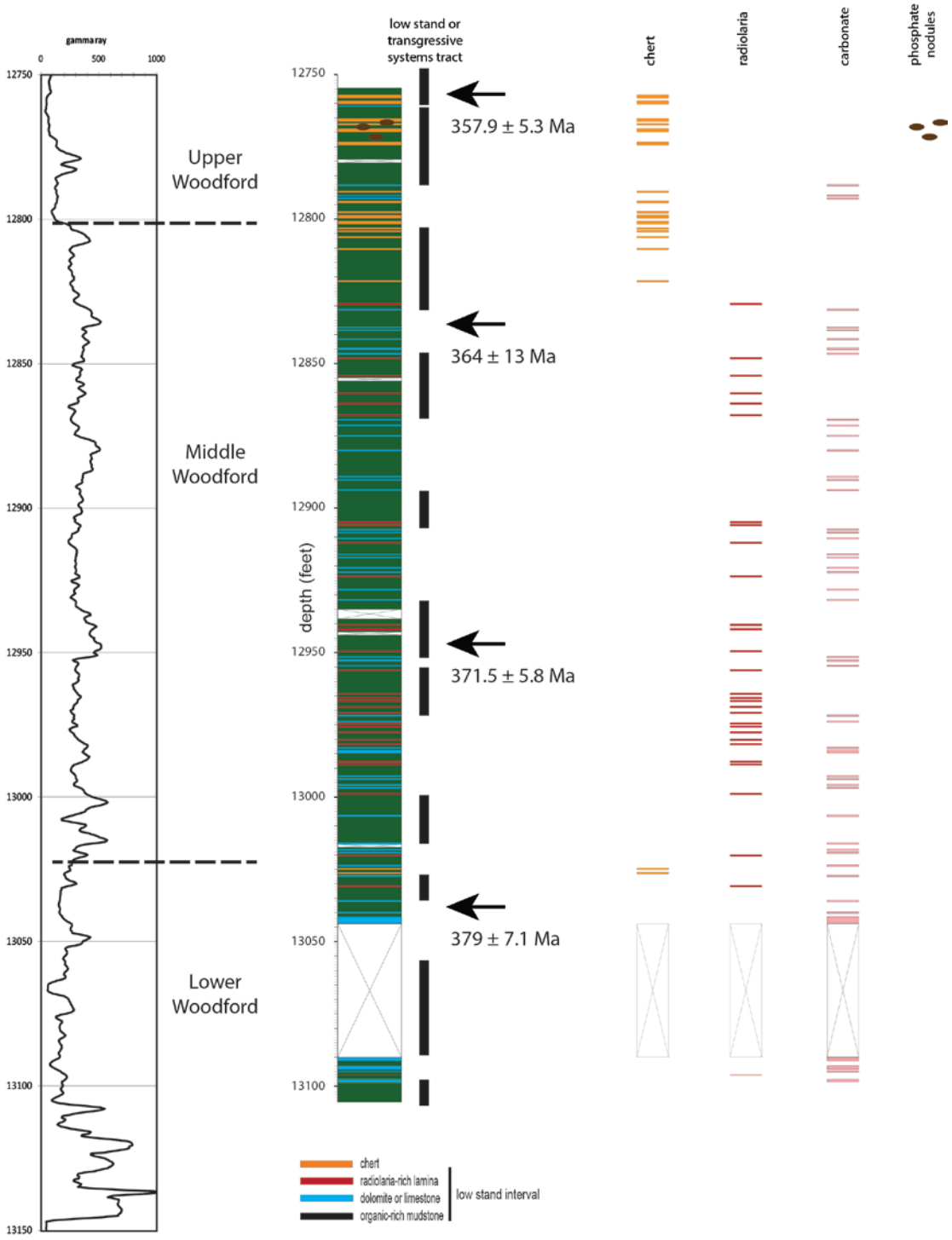

Figure 4. Description of the RTC #1 core, Pecos County. Occurrences of non-mudstone facies (chert, radiolarian-rich laminae, carbonate beds, phosphate nodules) are highlighted in the four righthand columns, with thicknesses exaggerated for visibility. Black bars indicate intervals without carbonate beds, interpreted as low stand / transgressive intervals.

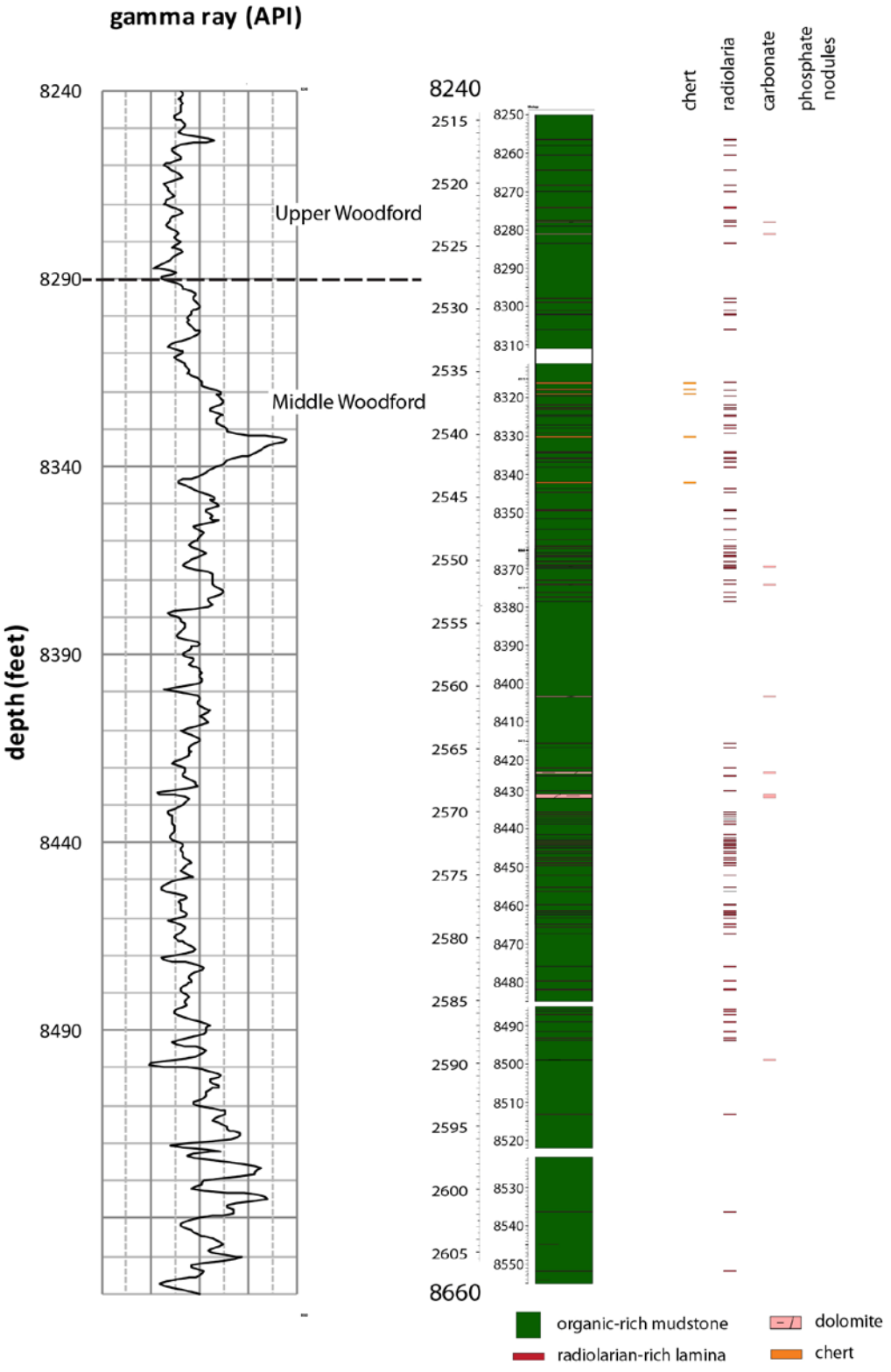

Figure 5. Description of the KCC 503 core, Winkler County. Symbols as in Figure 4.

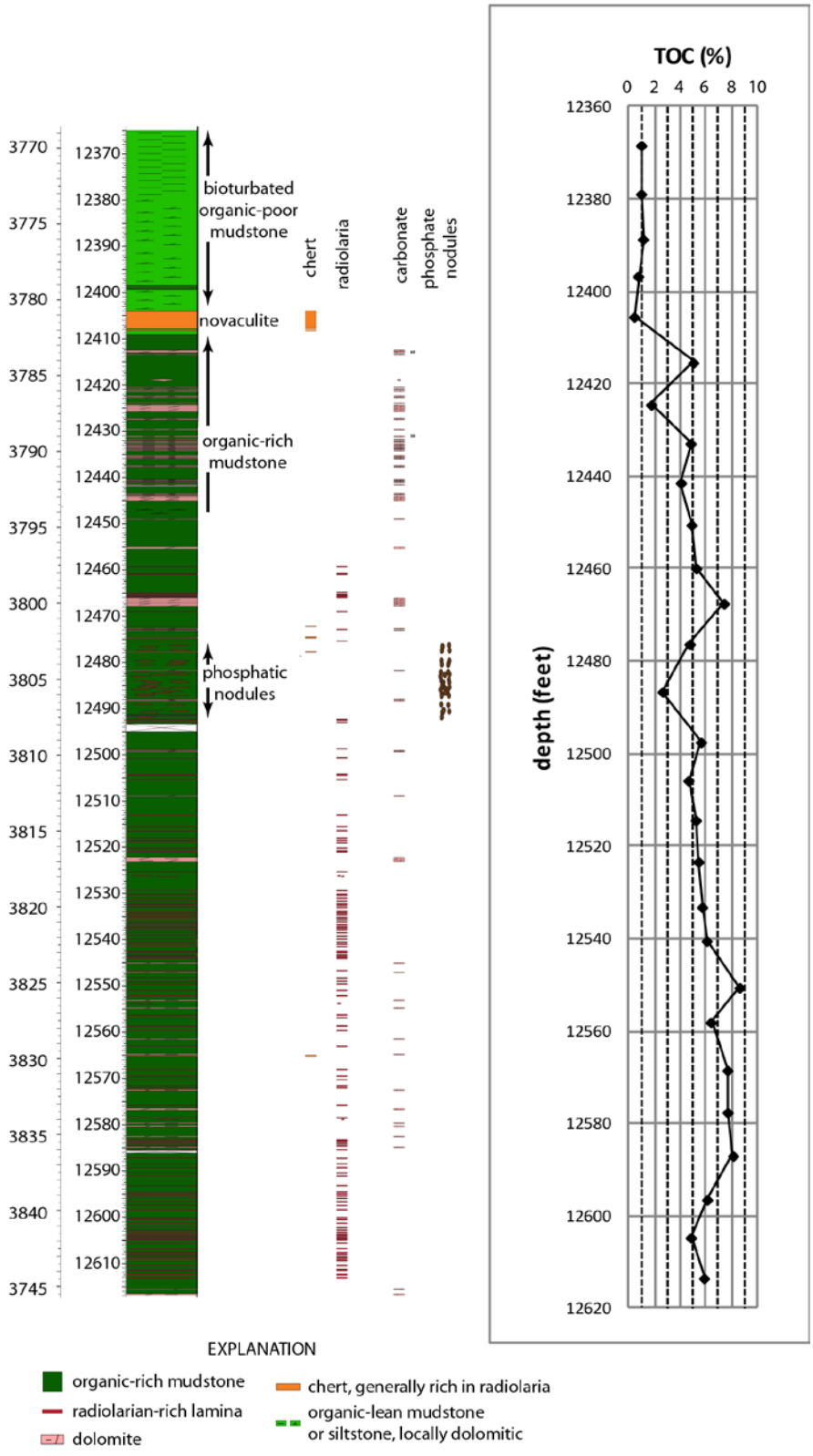

Figure 6. Description of the MBF core, Reeves Co. Symbols and description as in Figure 4.

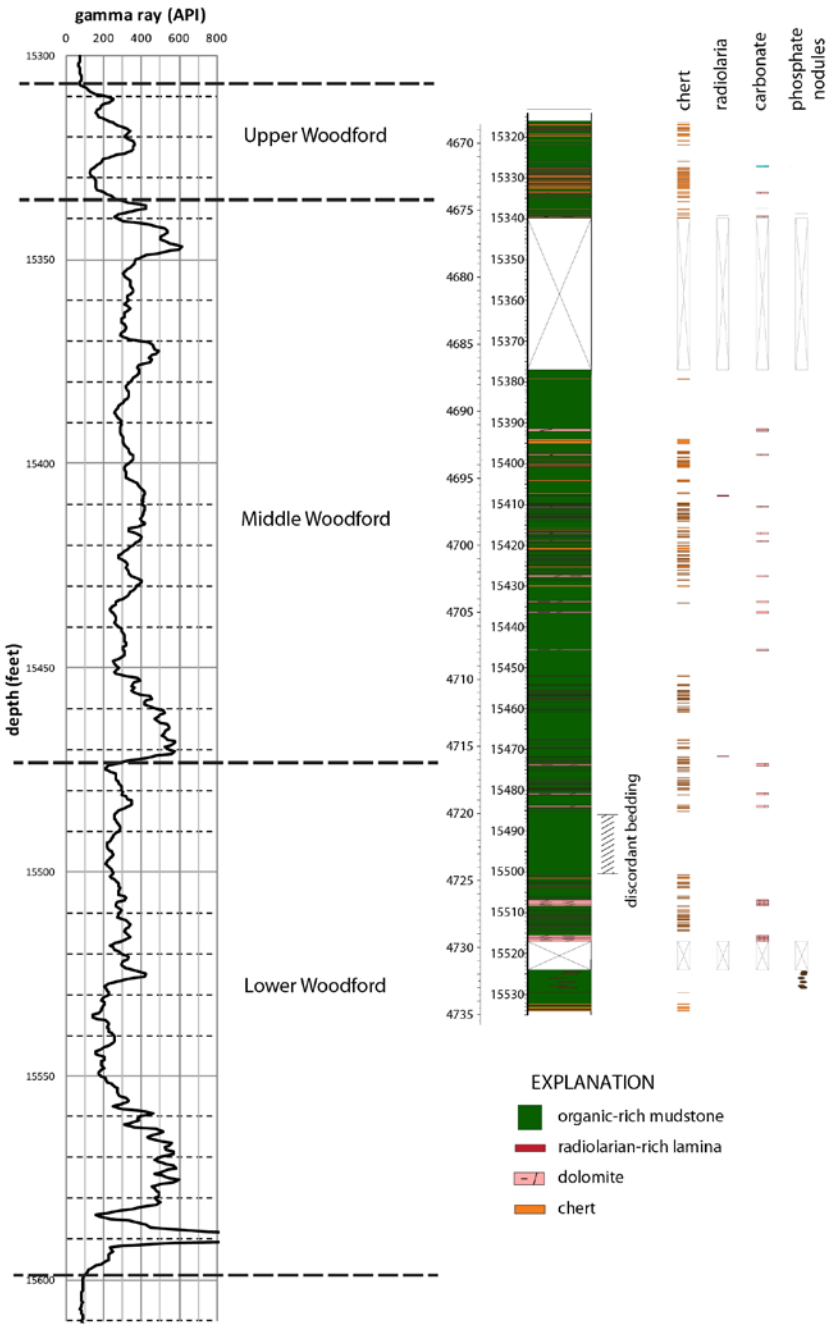

Figure 7. Description of the La Escalera B55 core, Winkler Co. Symbols and description as in Figure 4.

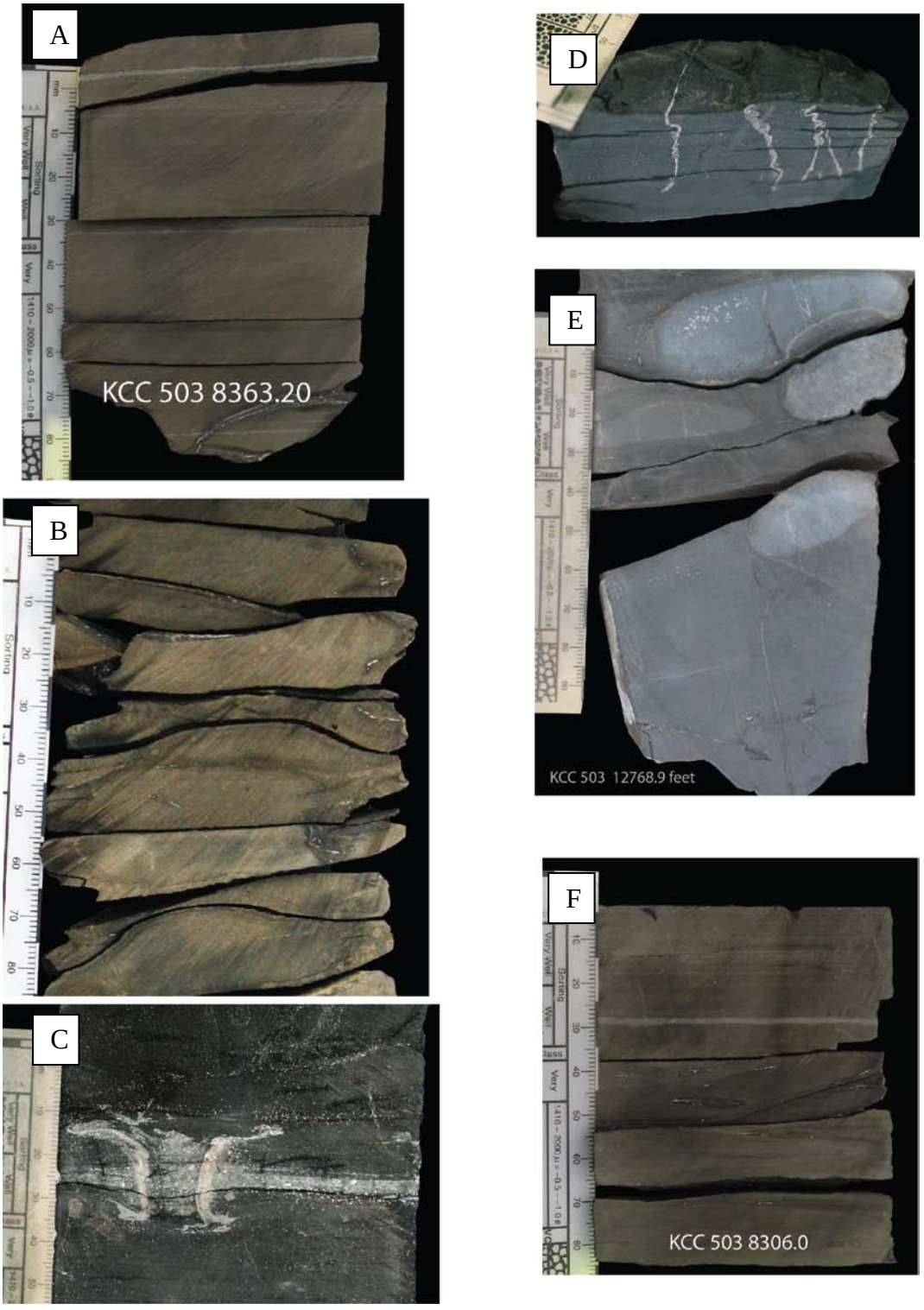

Figure 8.. Core photographs. A. Well-laminated mudstone. B. Massive or porrly laminated mudstone. C. Possible fluid escape structure. D. Synerisis cracks. E.Phosphate nodules in organic-rich mudstone. F. Radiolarian-rich lamina in laminated mudstone.

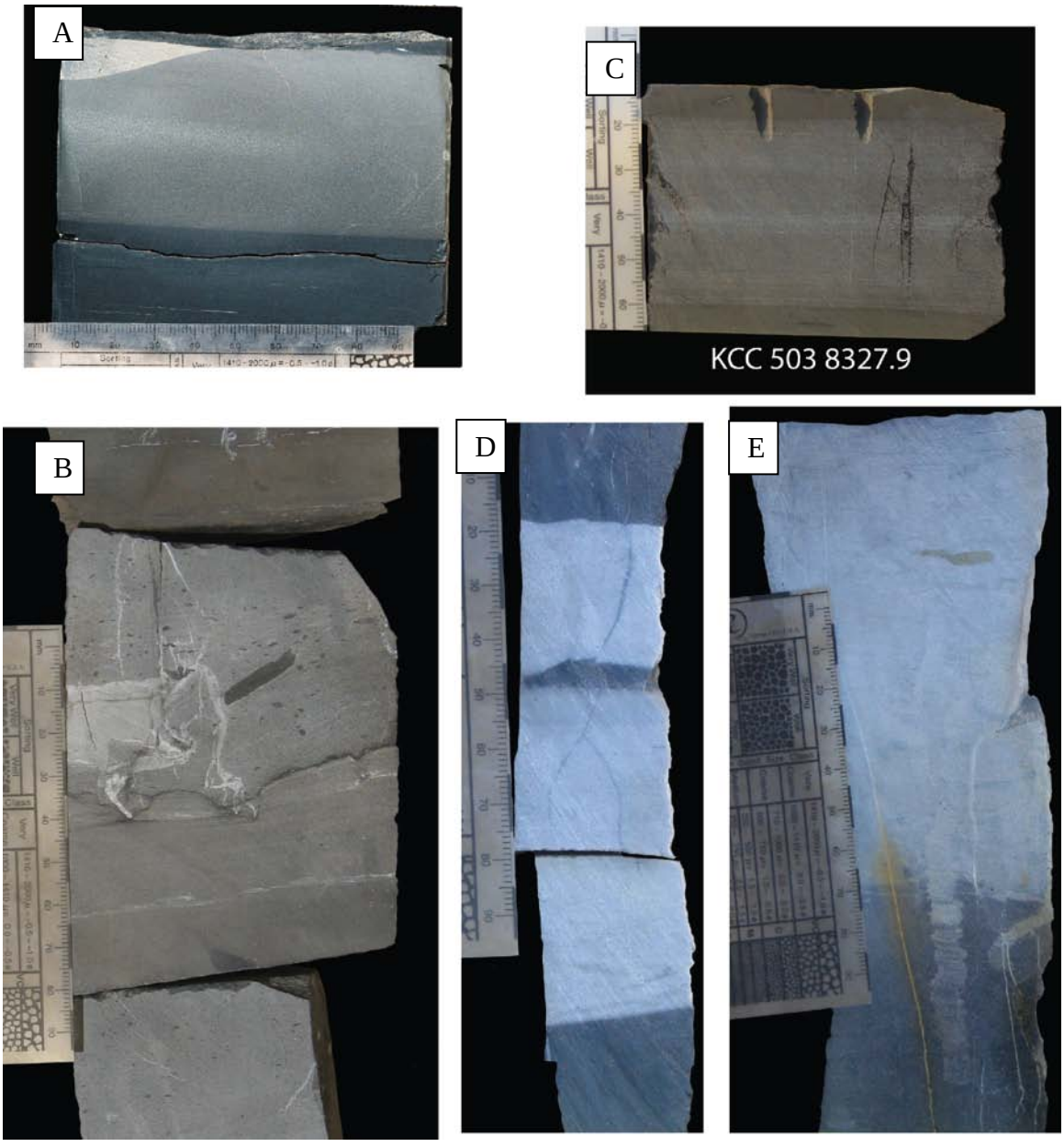

Figure 9. Core photographs. A. Dolomite bed. B. Dolomite bed with mudstone rip-up clasts. C. Chert bed. D. White and black novaculite. E. Bioturbated mudstone with large Teichichnus burrow.

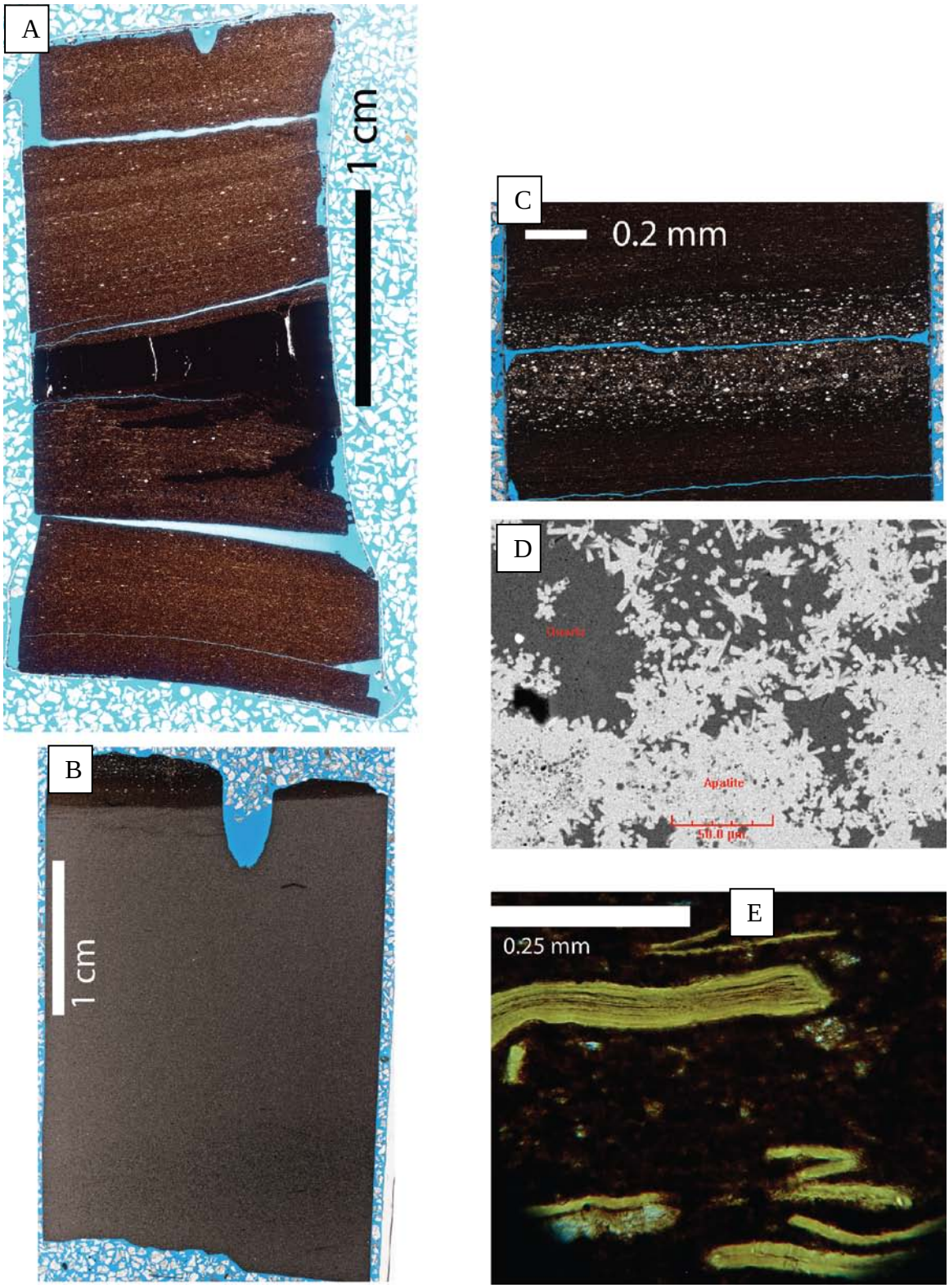

Figure 10. Thin section photographs. A. Laminated organic-rich mudstone. B. Dolomite bed. C. Radiolarian-rich lamina. D. Phosphate nodule. E. Tasmanites cysts in an organic-rich mudstone.

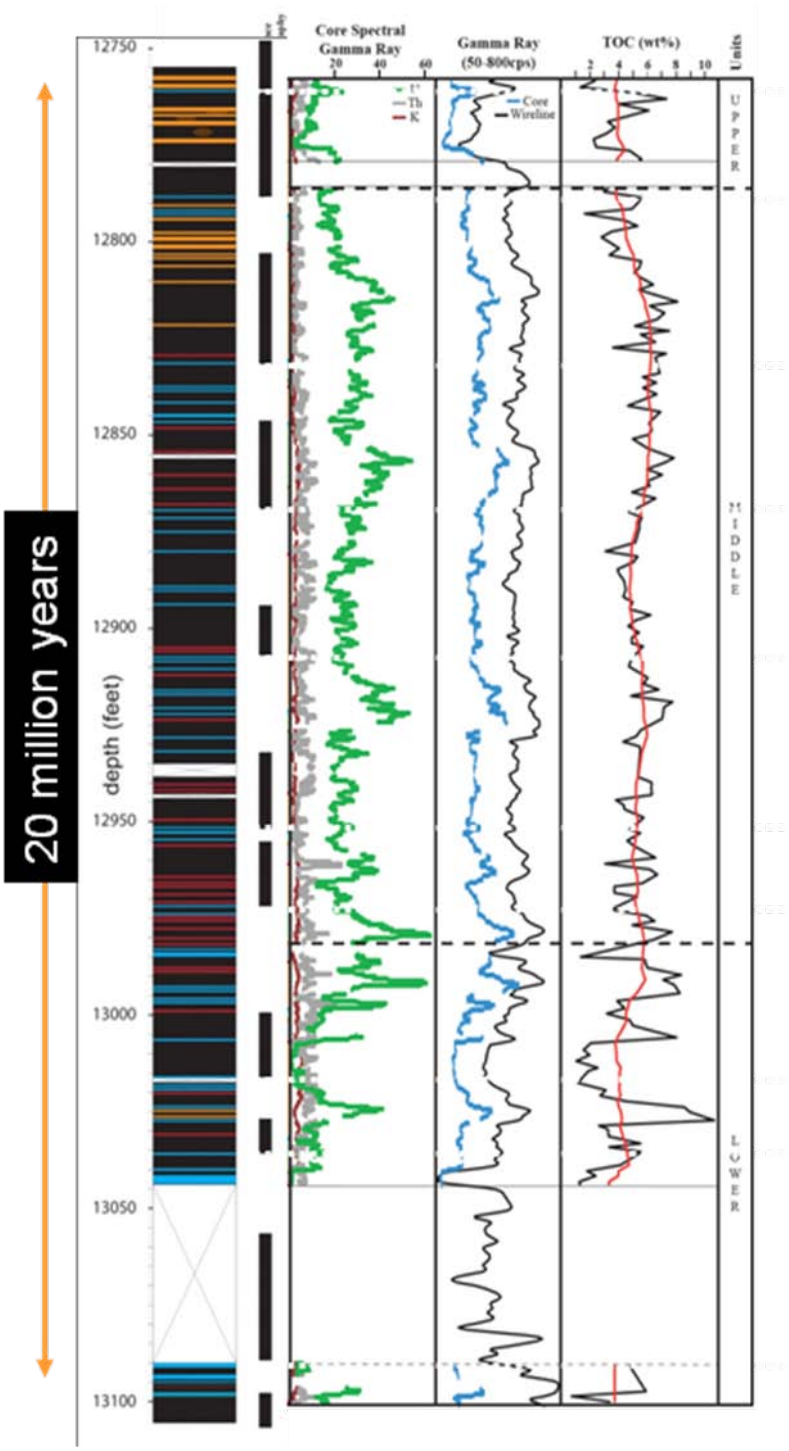

Figure 11. Description of the RTC#1 core, with core gamma (left track), total core gamma and wireline gamm (center track) and TOC (right track). The black bars represent interpreted low stand and transgressive systems tracts. In the core gamma data, brown represents potassium, grey thorium and green uranium. The red line in the TOC track represents a moving average over a 9 meter (30 feet) sliding window.